

THE UNSTEADY WAKE FROM A BODY MOVING NEAR AN INTERNAL LAYER

J.K.E. Tunaley¹

ABSTRACT

Unsteady wakes can be produced as a result of quasi-sinusoidal ship motion, by the ship's screws and by the reflection of ambient waves especially from the bow section of a ship hull. Unlike a steady wake, such as the Kelvin wake, the waves of an unsteady wake are not stationary in the reference frame of the source distribution. Such wakes might be important for the detection and classification of the vessel producing them; indeed surface ship wakes are common in radar imagery from space-borne radar. This paper describes the theory for the crest patterns for unsteady waves on a discrete internal layer and at the surface. Examples of patterns are presented for various cases. The drag produced by the production of an internal wave wake depends on the rate of production of momentum in the wake waves. This is compared to the energy carried away by the waves.

1. INTRODUCTION

THE WAKE from a vessel moving on or beneath the sea surface can often be seen in satellite-borne radar images of the ocean. Wakes can be used to aid the detection of a ship and for classification purposes. Whatever the sensor type, a consideration of the hydrodynamics of wake production is necessary to interpret the wake. Many types of wake can be created, such as the turbulent wake and the Kelvin wake of surface gravity waves. Here internal waves are considered and especially the case of unsteady internal wave wakes: the steady internal wake is a particular case in this class. The intention of this paper is to provide a framework for their examination and to describe some of their properties. As will be seen, the treatment to a large extent includes surface gravity waves as a special case.

The water in the ocean often exhibits small spatial variations. Its density is roughly horizontally stratified and fluctuates as a function of depth due to changes in salinity and temperature. Internal waves can propagate in three dimensions within the layers. In the case of ships, the waves that are generated often have a long wavelength comparable to the depth of a layer and there is considerable justification for simplifying the model. A single discrete layer corresponding to an abrupt change in

fluid density is adopted. This should have the advantage of illustrating many of the principal effects while the treatment remains reasonably transparent.

The depth of internal layers in the ocean typically lies in the range of a few metres to 200 m and the change in density at an internal interface varies with location, latitude and season. Near estuaries, there can be a change of density across an interface of about one percent while, in the open ocean in the tropics during summer the change is less, say 0.4 percent (Pickard and Emery, 1990).

A steady wake is generated by a perturbation that is constant in time within the reference frame of the ship. For the Kelvin wake, this perturbation arises from the flow of water around the hull. As a direct result of this, the wave pattern in the wake is also stationary in the ship frame. In contrast, unsteady wakes are generated by unsteady sources in the ship frame and similarly the wave patterns are unsteady. Unsteady wakes can be created by quasi-sinusoidal oscillations due to ship motions, the propeller and ambient waves reflected from the hull. However, the source terms are treated as exactly sinusoidal because the theory is based on the assumption of linearity and, at least in principle, any disturbance can be constructed from a sum of Fourier components.

Previous work on unsteady wakes seems to have focussed on surface waves. Crest patterns for unsteady surface wakes are illustrated by Wehausen and Laitone, 1960, but there has been some difficulty matching the crest patterns near the wake edge where there is a caustic. The calculation of the crest pattern is important for an appreciation of the wake appearance and is a first step

¹ London Research and Development Corporation, Ottawa, Canada, K0A 1L0. URL: <http://www.london-research-and-development.com/>

towards a full simulation of the wake from a ship. Simulations of the wave heights in an unsteady wake of surface gravity waves have been described by Tunaley, 1998.

Apart from their variation in time, unsteady wakes can exhibit a variety of features. For example, if the source of the wake is travelling very slowly, it is to be expected that waves can precede the ship as they propagate outwards in a roughly circular pattern. At moderate and high ship speeds there should be transverse and diverging waves. A practical wake is usually confined to a V-shape and its angle will change as a function of the parameters including the source frequency. The V-wake is the wake of interest here rather than the case of waves preceding the ship.

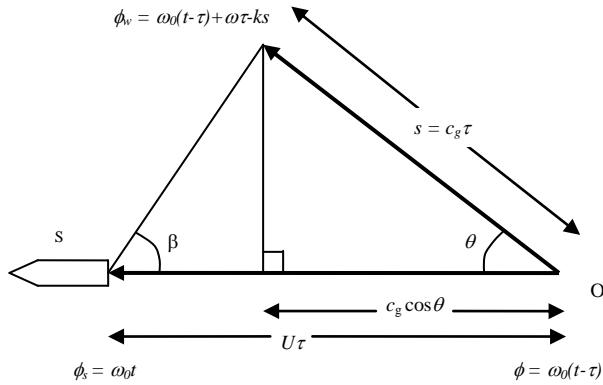


Fig. 1 Wake Geometry

The crest pattern is determined wholly by the dispersion relation for the waves and this involves the angular wave frequency, ω , and the angular wave vector, k . For an interface at depth h in an infinitely deep ocean where water of density ρ_1 overlies water of density ρ_2 , the dispersion relation can be found by assuming a velocity potential, Φ . This is of the form of a traveling wave in the horizontal direction and exponential in the vertical direction, and applying the appropriate boundary conditions at the free surface and at the internal layer (Crapper, 1967, or for the boundary conditions see Wehausen and Laitone, 1960) yields:

$$D(\omega, k) \equiv (\omega^2 - gk) \left(\omega^2 - \frac{\rho_2 - \rho_1}{\rho_1 + \rho_2 \coth(hk)} \right) = 0 \quad (1)$$

where g is the acceleration due to gravity. The first term in parentheses corresponds to surface gravity waves while the second corresponds to internal waves. Surface waves are dispersive and the internal wave propagation is also dispersive except for large wavelengths compared with

the depth of the layer. It is also worth noting that, if the upper fluid boundary condition is modified so that no surface waves are permitted, the result for internal waves is the same but the first term in parentheses (corresponding to surface waves) is absent.

2. THEORY

The wave vectors of the waves from a stationary oscillating source can be found from the dispersion equation in (1) and the crest pattern is in the form of circles concentric with the source. More generally, as a source moves horizontally at constant velocity, U , it creates a train of disturbances, which propagate radially outwards from the points at which they were created. This is illustrated in Fig. 1 which represents the unsteady wake and is analogous to the steady situation described by Keller and Munk, 1970.

The phase, ϕ_w , of the wave at a point in the wake can be deduced from Fig. 1:

$$\phi_w = \omega_0(t - \tau) + \omega\tau - ks, \quad (2)$$

where ω_0 is the angular frequency of the source, t is the time, τ is the time interval over which the wave has been propagating and s is the distance traveled by the wave. Maximum wave amplitudes will occur when the rate of change of phase with respect to k is zero: there will be a tendency for a group of waves to interfere constructively. Applying this stationary phase condition to (2) merely implies that $s = c_g\tau$, where the group velocity, c_g , is obtained from the dispersion relation by differentiation of ω with respect to k . Noting that the phase velocity, c , is just ω/k , (2) can be rearranged to yield:

$$\tau = \frac{\phi_s - \phi_w}{\omega_0 - k(c - c_g)}, \quad (3)$$

where ϕ_s is the phase of the source equal to $\omega_0 t$. In principle, the numerator can be positive or negative but to eliminate unphysical situations in which waves propagate inwards from infinity, $\tau > 0$.

The frequency of the waves in the water is related to the source frequency by the Doppler relation:

$$\omega_0 = \omega - kU \cos \theta, \quad (4)$$

where θ is the angle between the wave vector and the source track. This can be rearranged yielding:

$$\cos \theta = \frac{c}{U} - \frac{\omega_0}{kU}. \quad (5)$$

Now c can be found from the dispersion equation so that $\cos \theta$ can be calculated as a function of k . A snapshot

of the pattern for a single crest can be established by setting the numerator of (3) to some constant. Thus the time τ can be found for each value of k along a crest. Furthermore the position of this crest can be determined from Fig. 1:

$$\begin{aligned} x &= (U - c_g \cos \theta) \tau \\ y &= c_g \sin \theta \tau \end{aligned} \quad (6)$$

where x is a horizontal coordinate directed astern of the ship and y is a transverse coordinate. In effect, k can be regarded as a parameter tracing out each crest.

The phase at a crest remains constant as the pattern evolves with time. Since both x and y are proportional to τ , the individual crest shapes, separated by a phase difference of 2π , are identical except for a scale transformation and, as the pattern evolves, each crest moves so that it takes the place of another.

It is important to notice that in general there will be contributions to the wake from both positive and negative source frequencies. For example, a source that varies in time as a real cosinusoid can be decomposed into two complex exponential terms so that there will be equal contributions from both positive and negative frequencies. This gives rise to two separate wake components which in a linear theory are superposed. However, the two wake components will usually not be excited to an equal extent except when $\omega_0 = 0$, in which case the wake is steady and the two wake components coalesce.

In the frame of the source, the crest pattern of the *steady* wake is stationary. This is because $U \cos \theta = c$: the velocity of the crests matches the component of the source velocity along the wave vector and translations parallel to the crests are irrelevant. This is not the case for unsteady wakes, as can be seen from (5), so that the crest patterns will appear to move at different speeds. This can result in complicated wave patterns due to interference between the two wake components.

The principal part of the algorithm for calculating a single crest pattern can be summarized in the form of pseudo-code as follows²:

```

SET the source frequency,  $\omega_0$ , its speed,  $U$ , and internal
layer parameters ( $h, \rho_1, \rho_2$ );
SET the value of the relative phase ( $\phi_s - \phi_w$ ) to  $2\pi$  (or a
multiple of this);
FOR (a wide range of values of  $k$ ) DO {
  Calculate the phase and group velocities ( $c, c_g$ ) from
  the dispersion relation in (1);
  Calculate the propagation time,  $\tau$ , from (3);
  IF ( $\tau < 0$ ) {
    Change the sign of the relative phase;
  }
}

```

² Details, including resolution of a possible ambiguity, will be provided in another paper.

}

Calculate the cosine of the angle of the propagation vector, $\cos \theta$, from (5);

Calculate the x and y coordinates of the crest corresponding to the current value of k using (6);

3. CREST PATTERNS

In the following it is assumed that the fractional change in fluid density across the internal interface, δ , is small.

By a process of normalization, the crest patterns for surface gravity waves can be reduced to a one-parameter family: the maximum wake angle can be described as a function of a reduced source frequency. Only two parameters (Ω_0 and H) are required for internal gravity waves if the following normalization is adopted:

$$\begin{aligned} \Omega &= \frac{\omega U}{\delta g}, \quad \Omega_0 = \frac{\omega_0 U}{\delta g}, \quad \kappa = \frac{k U^2}{\delta g}, \\ X &= \frac{x \delta g}{U^2}, \quad Y = \frac{y \delta g}{U^2}, \quad H = \frac{h \delta g}{U^2}, \\ T &= \frac{\tau \delta g}{U} \end{aligned} \quad (7)$$

For example the dispersion relation for internal waves becomes:

$$\Omega^2 = \frac{\kappa}{1 + \coth(\kappa H)}. \quad (8)$$

The reduced phase velocity, $C = c/U = \Omega/\kappa$, while the reduced group velocity, $C_g = c_g/U = d\Omega/d\kappa$, is given by

$$C_g = \frac{C}{2} \left(1 + \frac{\kappa H e^{-\kappa H}}{\sinh(\kappa H)} \right). \quad (9)$$

When κH is very large, the denominator in the dispersion equation approaches two and the dispersion relation resembles that for ordinary surface waves. Reference to (9) shows that the group velocity approaches half the phase velocity as expected. When κH is very small, the group velocity approaches the phase velocity and the propagation is dispersionless with a normalized phase (and group) velocity $C = c/U = \sqrt{H}$, which in fact is the maximum velocity of internal waves in the fluid.

To classify the various patterns it is helpful to calculate a family of curves showing the maximum wake angle as a function of the normalized source angular frequency, Ω_0 , for different values of the normalized internal layer depth, H . This is shown in Figs. 2 and 3 in which the maximum half angle of the wake is plotted against the logarithm to the base 10 of the normalized angular frequency: Fig. 2 applies to positive frequencies and Fig. 3 to negative frequencies. The calculation is based on finding the angle β within the wake (see Fig. 1) using the algorithm described in the previous section and

then determining the maximum value of this wake half angle β .

When $H = \infty$, (or 1000 in this case) the curves resemble those presented by Lighthill, 1980. When $H \gg 1$, the internal layer is effectively deep; the wake pattern resembles that for surface gravity waves. When H is large and $\Omega_0 = 0$, a Kelvin wake is produced with the well known half angle of 19.47 degrees. As H decreases towards one, the angle of *steady* wakes increases and then, as H falls below one, the *steady* wake angle decreases. When $H < 1$, an upper limit to the wake half angle is provided by the maximum normalized wave velocity which is \sqrt{H} : this limiting wake half angle is just equal to $\sin^{-1}(\sqrt{H})$.

When Ω_0 is positive and $H > 1$, the wake angle first tends to increase with increasing source frequency. There is then a gap in the curves of Fig. 2. This is because at low source frequencies there exist waves that propagate ahead of the ship. These waves tend to have very long wavelengths which are not considered explicitly in the algorithm responsible for producing the graphs. However, in the gap these forward waves can affect the calculation and, to avoid confusion, all contributions have been omitted. As the source frequency increases beyond the gap, the wake angle, which at first is very wide, progressively narrows. At very high source frequencies, the curves for different values of H appear to coalesce.

The crest patterns can be calculated numerically using normalized parameters and the recipe in Section 2. For V-wakes there are basically two types of crest pattern. The first resembles the structure of divergent and transverse waves that is familiar from the Kelvin wake. An example of this structure is shown in Fig. 4 for an unsteady source with $\Omega_0 = 0.002$ and $H = 1.5$. The figure depicts a snapshot in time of a single crest for each of the two wake components corresponding to positive and negative frequencies. It applies to a time when the source at the origin is at its maximum amplitude and the phase of the crest relative to that of the source is 2π . Other crest locations can be calculated by multiplying the coordinates of the crest by integer values. Where the divergent and transverse waves meet at the wake component edges, there are likely to be caustics of cusp waves.

When the source frequency is positive, this type of structure appears at low source frequencies below the critical frequency at which there are waves preceding the source and for which $H > 1$. It also appears for negative frequencies for all values of H . An evaluation of the velocities of the waves shows that, to an observer on the ship, the positive frequency wake component appears to travel towards the ship while the negative frequency component appears to move away.

When $H < 1$, the source speed is always greater than the maximum velocity of the internal waves. Therefore

there can be no waves preceding the ship. For negative source frequencies this is also the case whatever the (positive) value of H . Thus for $H < 1$ there are no gaps in the curves of Fig. 2 and none in Fig. 3 for all H .

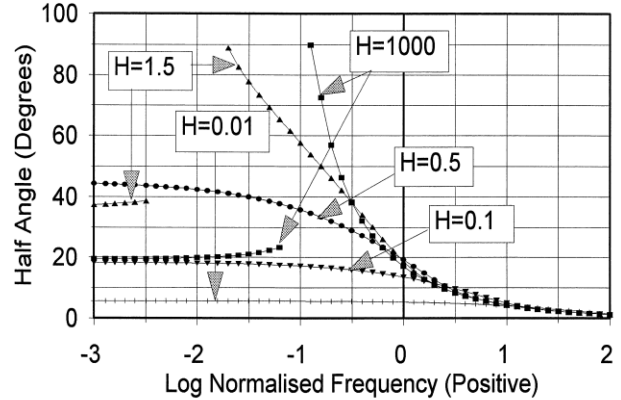


Fig. 2 Wake maximum half angle for positive frequencies.

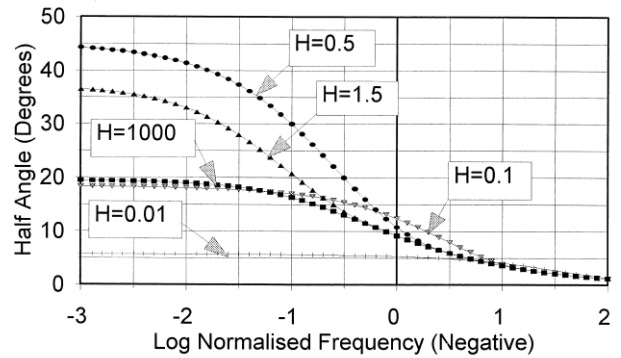


Fig. 3 Wake maximum half angle for negative frequencies.

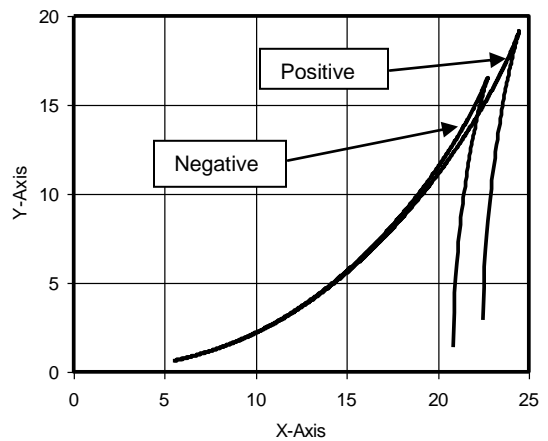


Fig. 4 Crest patterns for $H = 1.5$, $\Omega_0 = 0.002$.

Above the critical source frequency, the form of the crest pattern for the positive frequency component changes to a second type of solution while that for the negative component still resembles the Kelvin wake. The general form of the crest pattern is illustrated by an example for $H = 0.5$ and $\Omega_0 = 1.0$ in Figs. 5 and 6 for positive and negative frequencies respectively. The crests exhibit both transverse and divergent waves but with a different structure from the Kelvin wake. Because $H < 1$, the wake must be confined to a half angle less than 45 degrees (see also Fig. 2), which is certainly the case.

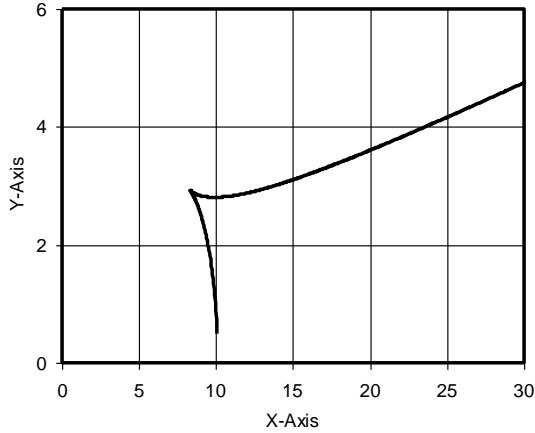


Fig. 5. Crest pattern for $H = 0.5$, $\Omega_0 = +1.0$.

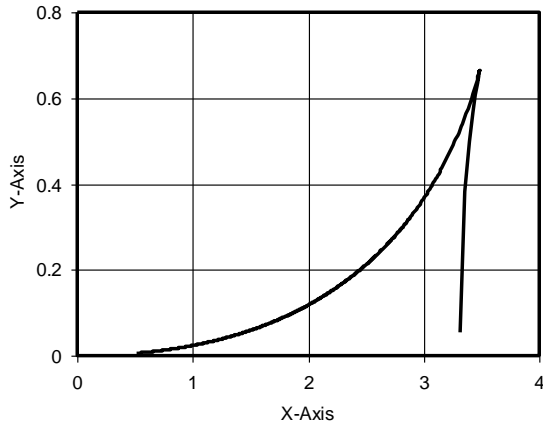


Fig. 6. Crest pattern for $H = 0.5$, $\Omega_0 = -1.0$.

That part of the crest pattern corresponding to the arc in Fig. 5 can be observed when a large water bird is startled and paddles away from the observer.

A further examination of the wake indicates that both crest components corresponding to positive and negative frequencies appear to move away from an observer on the ship.

It is also worth noting that, when $H < 1$ and $\Omega_0 \rightarrow 0$,

corresponding to a *steady* wake, the two wake components coalesce into a pattern in which the transverse waves of the positive frequency component go to the origin while those of the negative frequency component go to infinity. The result is a wake consisting of purely divergent waves.

The patterns and strengths of waves and their velocity fields at the ocean surface are often of more interest than those of the waves at the internal interface. Since it is usually assumed that the velocity potential is of exponential form (see ahead to equation (12) or refer to Lighthill), any perturbations of the internal layer tend to be reduced at the surface by an exponential factor e^{-kh} . This implies that the small wavelength waves will be attenuated at the surface and long wavelength waves will predominate. As for the Kelvin wake, the transverse waves of an internal wave wake have the longest wavelengths and so these should often be the main feature of the surface manifestation of an unsteady internal wave wake.

4. ENERGY AND MOMENTUM

A consideration of the energy and momentum in the waves is important for the estimation of the wave resistance attributable to an unsteady wake and for the damping of the source terms (such as in heaving and pitching of a ship). The waves in the wake carry both energy and momentum from the source. When the wake is steady, such as when it arises from the movement of fluid around the ship's hull, the energy carried away by the waves must be produced at the expense of the kinetic energy of the ship or by the propulsion system. It can be interpreted as a wave-making resistance. In fact various authors have calculated the wave-making resistance from the Kelvin wake (the principles are discussed by Lighthill, 1980). When the wake is unsteady, the energy in the waves can be produced not only as a result of drag on the ship but also by damping of the source itself: the heaving motion of a ship can result in both a drag additional to that from the Kelvin wake and in a damping of the heaving motion.

To calculate the drag component, the rate of production of the component of momentum in the direction of the ship should be calculated. This is numerically equal to the drag force by Newton's laws. The momentum of a wave is a second order quantity in the wave amplitude, ζ , and therefore, on a strictly linear theory, it is zero. Lighthill, 1980 (see exercise 1 on p 249), points out that it is directly related to the Stokes drift. Thus it may be calculated by considering the orbital motion of fluid elements as they move through points with differing velocity potential. Lighthill, 1980, finds that for surface gravity waves, the momentum per unit

horizontal area, p , is:

$$p = \frac{1}{2} \rho \omega \zeta^2. \quad (10)$$

For internal waves, the calculation of the Stokes drift can be accomplished in two steps. Below the internal interface, the velocity potential falls exponentially and the orbits of fluid elements are approximately circles. Therefore the momentum per unit area contributed by all the fluid below the interface is given by an expression similar to that for surface gravity waves:

$$p = \frac{1}{2} \rho_2 \omega \zeta^2, \quad (11)$$

where ζ is now the internal wave amplitude. Above the interface the orbits are ellipses and this requires a new calculation.

Above the interface, the velocity potential is assumed to be of the form:

$$\Phi = (Ae^{kz} + Be^{-kz}) \cos(\omega t - kx). \quad (12)$$

This permits the horizontal and vertical components of the fluid velocity to be calculated in terms of the constants A and B. The fluid element positions can be obtained by integration of the velocity with respect to time. However, in the integration, x and z are treated as constant. The horizontal distance traveled in one orbit can then be found to second order by substitution of the first order results in the velocity potential and performing a further integration of the velocity over a single period.

There are two contributions to this corresponding to variations in the velocity potential as a function of z and as a function of x . (In the case of simple surface gravity waves these contributions are equal.) The result for internal waves is that, at depth z , the Stokes drift per period, d , is given by:

$$d = \pi \frac{k^3}{2\omega^2} (A^2 e^{2kz} + B^2 e^{-2kz}). \quad (13)$$

The average drift per period over that part of the ocean above the interface can be found by integrating over z . Multiplying by the frequency, $\omega/(2\pi)$, gives the average drift velocity so that the momentum can be found. This gives the momentum of the waves in the fluid above the interface:

$$p = \frac{1}{2} \rho_1 \frac{k^2}{\omega} ((1 - e^{-2kh})A^2 - (1 - e^{2kh})B^2). \quad (14)$$

The remaining part of the calculation can be simplified if it is noted that the velocities associated with internal waves are greatest near the interface and tend to fall rapidly away from it. If the boundary condition at the free surface is set so that no vertical surface displacement is permitted, then the z -component of the velocity at the surface must be zero and it can be shown from equation (12) that $A=B$. Similarly, at the interface, the boundary condition can be written:

$$\frac{\partial \zeta}{\partial t} = \frac{\partial \Phi}{\partial z}. \quad (15)$$

Thus adding the wave momentum per horizontal area from above the interface to that from below it (see (11)) gives:

$$p = \frac{\omega \zeta^2}{2} (\rho_1 \coth(kh) + \rho_2). \quad (16)$$

This can be simplified using the dispersion equation (1) giving:

$$p = \frac{1}{2} (\rho_2 - \rho_1) \frac{gk}{\omega} \zeta^2 = \frac{1}{2c} (\rho_2 - \rho_1) g \zeta^2. \quad (17)$$

This result can be compared with the total mechanical energy in the waves, namely the sum of the kinetic and potential energies. It has been noted by Lighthill, 1980, that in a linear system energy is transferred from kinetic to potential and back in each oscillation and that the average kinetic and potentials are equal. Therefore the total energy is equal to the maximum kinetic or maximum potential energies. This implies that, when no surface waves are permitted, the total energy per horizontal area, E , is equal to the maximum potential energy per unit area at the internal interface, i.e.

$$E = \frac{1}{2} (\rho_2 - \rho_1) g \zeta^2. \quad (18)$$

5. WAVE-MAKING DRAG

The theory in Section 2 implies that for each point in the wake there exists a limited number, n , of wave vectors k that satisfy the stationary phase condition and other constraints. These are the same wave vectors employed in the crest shape calculations and typically correspond to divergent and transverse waves of the two wake components. If a spatial distribution of sources has been determined, it can be decomposed into Fourier components and, from these, the amplitude and direction of the waves at a point in the wake can be determined (e.g. Tuck et al, 1971). To find the rate of production of wake momentum or wake energy, an integration of the momentum or energy can be performed along a strip of width $(U - c_g \cos\theta) dt$ running perpendicular to the source track (compare Milne-Thomson, 1968, pp 437, for example). The position of this strip astern of the sources is not important because, with the exception of caustic regions (small in the far wake), the wave amplitude decreases as distance to the power $-1/2$ while its square falls inversely with distance. On the other hand the width of the wake region increases as the distance.

The rate of production of the component of momentum parallel to the source track, which is the wave-making resistance, R , is given by

$$R = \frac{dp}{dt} = \sum_n \int_{-\beta_0}^{\beta_0} \frac{1}{2} (\rho_2 - \rho_1) \frac{g}{c_n} \zeta_n^2 \times (U - c_g \cos \theta) \cos \theta r \cos \beta d\beta \quad (19)$$

where β is the angle within the wake (see Figure 1) and $\pm\beta_0$ are the wake limits. In contrast, the rate of production of wake energy is given by

$$\frac{dW}{dt} = \sum_n \int_{-\beta_0}^{\beta_0} \frac{1}{2} (\rho_2 - \rho_1) g \zeta_n^2 \times (U - c_g \cos \theta) r \cos \beta d\beta \quad (20)$$

If all the wake energy can be attributed to wave-making resistance, $dW/dt = RU$. When $\omega_0 = 0$ and the wake is steady, equation (4) indicates that

$$\omega = kU \cos \theta. \quad (21)$$

By replacing c by ω/k in equation (19) and substituting from equation (21) it can be verified that energy and momentum considerations give the same drag, R . However, for unsteady wakes, this will generally not be true and the difference is related to damping of the source.

The $\cos\theta$ factor in the expression for the drag force in equation (19) can be negative. This occurs when Ω_0 is positive and it is larger than some critical value (which is a function of H) and represents the situation where the production of some component waves provides a propulsive force contribution.

6. SUMMARY

A simple numerical algorithm has been described from which the crest pattern for unsteady internal waves can be calculated. Different crest patterns can be produced depending on the parameters. For practical layer strengths, layer depths and for source speeds of a few metres per second, the surface manifestation of an internal wave wake will exhibit a small wake angle which becomes narrower as the source frequency rises. Unlike the typical steady internal wave wake for which $H < 1$ and which consists only of divergent waves, transverse waves can always occur with unsteady wakes. At the water surface, these are likely to be the prominent feature of the unsteady wake and produce a narrow oscillating pattern astern of the source.

The existence of a wake implies that there is a production of energy and momentum. The calculation of the energy in the wake is not sufficient to determine wave-making resistance except in the steady case but the production of linear momentum is directly related to the drag on the ship. It is noteworthy that, once momentum has been created in the water, it remains there until it is transferred to the air above the fluid, the ocean floor or the shore. Therefore it is unaffected by wave breaking.

This is in contrast to the wave energy which can be dissipated both by viscosity and by wave breaking as well as be affected by the action of the wind. Therefore wave momentum provides a more reliable indicator of drag than the energy. However, the wave momentum may be difficult to measure.

REFERENCES

- CRAPPER, G.D. 1967, Ship Waves in a Stratified Ocean", *J. Fluid Mechanics*, **29**(4), 667-672.
- KELLER, J.B. and W.H. MUNK 1970, Internal Wave Wakes of a Body Moving in a Stratified Fluid, *Physics of Fluids*, **13**(6), 1425-1431.
- LIGHTHILL, J. 1980, *Waves in Fluids*, Cambridge University Press.
- MILNE-THOMSON, L.M. 1968, *Theoretical Hydrodynamics*, Dover.
- PICKARD, G.L. and W.J. EMERY 1990, *Descriptive Physical Oceanography*, 5th Edition, Pergamon Press.
- TUCK, E.O., J.I. COLLINS and W.H. WELLS 1971, On Ship Wave Patterns and Their Spectra, *SNAME J. Ship Research*, 11-21, March, 1971.
- TUNALEY, J.K.E. 1998, Further Modifications to the DREO Ship Wake Algorithms, London Research and Development Report under DSS contract W7714-7-0075 for DRDC, Ottawa, March, 1998.
- WEHAUSEN, J.V. and E.V. LAITONE 1960, Surface Waves, *Handbuch der Physik, Vol XI, Fluid Dynamics III*, Springer Verlag, 1960.